Improved MRAS with stator and rotor resistance estimation for vector control of induction motors

Tran Dinh Cuong[1*], Phan Thanh Tai[1], Nguyen Thanh Quang[1], Phan Tran Dang Khoa[2]

[1]Power System Optimization Research Group, Faculty of Electrical and Electronics Engineering, Ton Duc Thang University, No.19 Nguyen Huu Tho Street, Tan Hung Ward, Ho Chi Minh City, Vietnam;
[2]Faculty of Electrical and Electronics Engineering, Ton Duc Thang University, No.19 Nguyen Huu Tho Street, Tan Hung Ward, Ho Chi Minh City, Vietnam.
[*]Corresponding author: trandinhcuong@tdtu.edu.vn
Received 30 Oct. 2025; Revised 6 Dec. 2025; Accepted 10 Feb. 2026; Published 25 Feb. 2026.
DOI: https://doi.org/10.54939/1859-1043.j.mst.109.2026.14-24

ABSTRACT

This research addresses the degradation of speed estimation accuracy in speed-sensorless induction motor drives that arises from temperature-dependent variations of stator and rotor resistances. These parameter changes significantly affect the Rotor Flux-Based Model Reference Adaptive System (RF-MRAS) observer, leading to reduced robustness and unstable operation under dynamic conditions. To mitigate this issue, an enhanced Field-Oriented Control (FOC) scheme is proposed, integrating an adaptive RF-MRAS observer with an online estimation mechanism for the stator resistance and a proportional inference approach for the rotor resistance. A complete induction motor model is formulated in the stationary α-β reference frame and subsequently transformed into the rotating d-q frame to facilitate the implementation of the vector control strategy. Simulation studies, conducted under both sudden step changes and gradual ramp variations of the motor resistances, verify that the proposed method significantly improves speed estimation accuracy and enhances overall system stability. Owing to its simple structure and low computational burden, the proposed approach is suitable for real-time embedded applications in modern sensorless motor drive systems.

Keywords: Induction motor; Field-oriented control; Speed sensorless; RF-MRAS; Resistance variation.

1. INTRODUCTION

Induction Motor (IM) drives continue to dominate in industrial and transportation applications due to their robustness, simplicity, and cost-effectiveness [1]. To achieve high performance comparable to DC and permanent magnet drives, the Field-Oriented Control (FOC) strategy is widely adopted, as it enables decoupled control of torque and flux in a rotating reference frame, thereby ensuring fast dynamic response and accurate steady-state regulation [2, 3].

In recent years, attention has increasingly turned to speed sensorless control of IM drives to eliminate mechanical speed sensors, which add cost, complexity, and reduced reliability [4, 5]. Among various estimation techniques, the study [6] proposed a method that uses a basic Phase-Locked Loop (PLL) combined with a simple machine model to reconstruct the Back-EMF and estimate rotor position and speed without a physical sensor. Besides, the model reference adaptive system (MRAS) has been one of the most popular solutions due to its simple structure, low computational burden, and good dynamic performance [7, 8]. For example, the research [9] reformulates the Reactive Power-Based MRAS (Q-MRAS) to ensure stability across all four quadrants of operation, while remaining independent of stator resistance and free of differentiation and integration operations. Another publication on controlling speed sensorless proposes an improved rotor flux estimation method for the Torque Model Reference Adaptive System (TMRAS) [10].

However, traditional MRAS estimators rely on the accuracy of machine parameters, particularly the stator resistance (R_s) and rotor resistance (R_r), which are sensitive to temperature

variations. When the squirrel-cage rotor motor operates under load or at high temperatures, the thermal increase in the stator winding and rotor bars results in significant changes in R_s and R_r. These parameter variations result in errors in rotor flux estimation, consequently deteriorating the accuracy of the estimated rotor speed and the stability of the overall sensorless drive [11]. Several studies have attempted to mitigate this problem. An application of the Current-Based MRAS (CB-MRAS) model for speed sensorless control [12] integrates a stator resistance estimation block that operates under varying operating conditions. Similar to paper [12], the authors in [13] also developed a CB-MRAS scheme to estimate R_s in real time. Although these methods improve accuracy, they often increase algorithmic complexity or require additional signal processing hardware. Moreover, these studies do not account for variation in rotor resistance.

More recently, hybrid adaptive observers and intelligent algorithms such as fuzzy logic, neural networks, and particle swarm optimization (PSO) have been introduced to estimate speed or compensate for parameter variations in sensorless IM drives [14-16]. Despite their promising results, these approaches often require substantial computational resources and are difficult to implement on embedded systems. Hence, there is still a need for a simple, robust, and computationally efficient solution that can maintain accurate estimation performance under thermal parameter variations.

To address these challenges, this paper proposes an improved speed sensorless FOC scheme based on the Rotor Flux-Based Model Reference Adaptive System (RF-MRAS), in which both stator and rotor resistances are adaptively estimated online. The stator resistance is calculated from the flux error between the reference model (voltage model) and the adaptive model (current model). In contrast, the rotor resistance is derived in proportion to the estimated stator resistance. The proposed adaptive observer is fully integrated into the FOC structure, allowing continuous parameter updating during operation without additional signal injection or complex computation.

2. THEORETICAL FOUNDATION AND DESIGN

2.1. Mathematical model

The squirrel-cage induction motor is modeled through the relationships among the state variables of stator voltage, stator current, rotor flux, and motor parameters [17]:

$$\begin{cases} \hat{u}_s = R_s \times \hat{i}_s + \left(\dfrac{L_s.L_r - L_m^2}{L_r} \right) \times L_s \dfrac{d\hat{i}_s}{dt} + \dfrac{L_m}{L_r} \times \dfrac{d\hat{\psi}_r}{dt} \\ 0 = -\hat{i}_s \times \dfrac{L_m R_r}{L_r} + \hat{\psi}_r \times \left(\dfrac{R_r}{L_r} - j\omega_r \right) + \dfrac{d\hat{\psi}_r}{dt} \end{cases} \tag{1}$$

The electromagnetic torque equation is shown in (2):

$$T_e = \frac{3}{2} \times \frac{L_m}{L_r} \times p \times \left(\psi_{r\alpha} \times i_{s\beta} - \psi_{r\beta} \times i_{s\alpha} \right) \tag{2}$$

The relationship between electromagnetic torque and load torque:

$$T_e = T_L + \frac{J}{p} \times \frac{d\omega_r}{dt} \tag{3}$$

2.2. Clarke-Park transformation

The three-phase induction motor in this study is modeled based on mathematical equations in the stationary reference frame. Therefore, the Clarke transformation from the abc reference frame to the stationary reference frame is required to connect the motor. The Clarke transformation is presented as follows:

$$\begin{bmatrix} \dot{X}_a \\ \dot{X}_b \\ \dot{X}_c \end{bmatrix} = \begin{bmatrix} 1 & 0 \\ -\frac{1}{2} & \frac{\sqrt{3}}{2} \\ -\frac{1}{2} & -\frac{\sqrt{3}}{2} \end{bmatrix} \times \begin{bmatrix} \dot{X}_\alpha \\ \dot{X}_\beta \end{bmatrix} \Leftrightarrow \begin{bmatrix} \dot{X}_\alpha \\ \dot{X}_\beta \end{bmatrix} = \frac{2}{3} \begin{bmatrix} 1 & -\frac{1}{2} & -\frac{1}{2} \\ 0 & \frac{\sqrt{3}}{2} & -\frac{\sqrt{3}}{2} \end{bmatrix} \times \begin{bmatrix} \dot{X}_a \\ \dot{X}_b \\ \dot{X}_c \end{bmatrix} \quad (4)$$

However, to implement rotor field-oriented control, it is necessary to transform the state variables from the stationary reference frame to the rotating reference frame:

$$\begin{bmatrix} \dot{X}_\alpha \\ \dot{X}_\beta \end{bmatrix} = \begin{bmatrix} \cos\theta & \sin\theta \\ \sin\theta & \cos\theta \end{bmatrix} \times \begin{bmatrix} \dot{X}_d \\ \dot{X}_q \end{bmatrix} \Leftrightarrow \begin{bmatrix} \dot{X}_d \\ \dot{X}_q \end{bmatrix} = \begin{bmatrix} \cos\theta & \sin\theta \\ -\sin\theta & \cos\theta \end{bmatrix} \times \begin{bmatrix} \dot{X}_\alpha \\ \dot{X}_\beta \end{bmatrix} \quad (5)$$

2.3. Speed sensorless field-oriented control considering the influence of motor resistance parameters

Figure 1 illustrates the FOC structure for a three-phase induction motor drive system without a speed sensor. The FOC principle controls the flux and torque components independently.

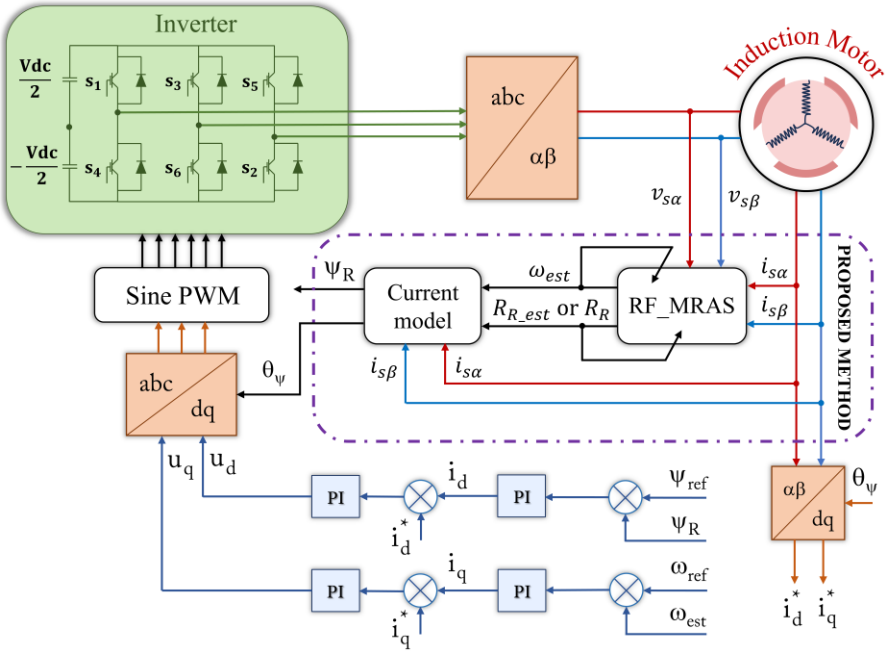

Figure 1. *Rotor field-oriented control scheme combined with an RF-MRAS estimator.*

The voltages u_d and u_q obtained from the FOC method are combined with the rotor flux angle to generate three-phase voltage signals. These voltage signals are then processed through Sinusoidal Pulse Width Modulation (SPWM) to produce the switching pulses for the inverter. The rotor flux angle is calculated using the current model described by equations (6) and (7).

The MRAS model consists of a reference model and an adaptive model. The reference model receives signals from the stator voltage and current measured by sensors. The reference model's output signal is the rotor flux. Moreover, this is an improved model as it incorporates an estimated stator resistance. Therefore, the reference model can also adjust itself. The equations of the reference model are expressed as follows:

$$\psi_{r\alpha}^{RM} = A \times \left[\int (u_{s\alpha} - R_{s\_est} \times i_{s\alpha}) dt - B \times i_{s\alpha} \right] \quad (6)$$

$$\psi_{r\beta}^{RM} = A \times \left[\int (u_{s\beta} - R_{s\_est} \times i_{s\beta}) dt - B \times i_{s\beta} \right] \quad (7)$$

Where: $A = \frac{L_r}{L_m}$; $B = \frac{L_s.L_r - L_m^2}{L_r}$

The adaptive model is constructed according to equations (8) and (9), which receive the current and speed signals as inputs. In speed sensorless drive applications, this speed corresponds to the estimated speed. Moreover, this is an improved model since it incorporates the estimated rotor resistance. Therefore, the adaptive model can automatically adjust itself based on the estimated speed and rotor resistance.

$$\psi_{r\alpha}^{AM} = \int \left(\frac{L_m \times R_{r\_est}}{L_r} \times i_{s\alpha} - \frac{R_{r\_est}}{L_r} \times \psi_{r\alpha}^{AM} - \omega_{r\_est} \times \psi_{r\beta}^{AM} \right) dt \quad (8)$$

$$\psi_{r\beta}^{AM} = \int \left(\frac{L_m \times R_{r\_est}}{L_r} \times i_{s\beta} - \frac{R_{r\_est}}{L_r} \times \psi_{r\beta}^{AM} + \omega_{r\_est} \times \psi_{r\alpha}^{AM} \right) dt \quad (9)$$

From the reference and adaptive models, the flux component errors are calculated using equation (10) and then fed into the PI controller described by equation (11). The PI controller's output provides the estimated speed.

$$\varepsilon_{\omega} = \psi_{r\alpha}^{AM} \times \psi_{r\beta}^{RM} - \psi_{r\beta}^{AM} \times \psi_{r\alpha}^{RM} \quad (10)$$

$$\omega_{r\_est} = K_p \times \varepsilon_{\omega} + K_i \times \int \varepsilon_{\omega} dt \quad (11)$$

In addition, equations (12)-(13) present the procedure for estimating the stator resistance based on the flux components and the stator current. Another PI controller adjusts the estimated stator resistance as the stator windings' temperature changes.

$$\varepsilon_{R_s} = \left(\psi_{r\alpha}^{RM} - \psi_{r\alpha}^{AM} \right) \times i_{s\alpha} + \left(\psi_{r\beta}^{RM} - \psi_{r\beta}^{AM} \right) \times i_{s\beta} \quad (12)$$

$$R_{s\_est} = K_p \times \varepsilon_{R_s} + K_i \times \int \varepsilon_{R_s} dt \quad (13)$$

As reported in the study [11], both the stator and rotor resistances vary proportionally with changes in motor temperature. Moreover, the temperature coefficients of the copper material (stator winding) and the aluminum material (rotor bars) are nearly the same, approximately 0.004 K^{-1}. Therefore, this study assumes that the estimated rotor resistance increases proportionally to the stator resistance and is calculated according to equation (14):

$$R_{r\_est} = k \times \frac{R_{s\_est}}{R_s} \times R_r \quad (14)$$

Where: k is the ratio representing the deviation between the temperature-induced increase of the stator and rotor resistances (assuming the stator resistance increases by 30% and the rotor resistance increases by 20%, then k=12/13=0.92308).

Regarding stability, the adaptive mechanism used in the proposed RF-MRAS follows the same structural form as classical MRAS estimators whose convergence has been rigorously proven in prior studies. The publication in [18] showed that MRAS schemes with PI-type adaptation satisfy Popov's hyperstability criterion, ensuring global convergence of the estimation deviation. Likewise, the research in [19] provided a unified MRAS framework and demonstrated that Lyapunov-based and Popov-based analyses lead to equivalent stable adaptive laws for rotor time constant identification. Since our RF-MRAS employs an identical PI-based mechanism structure based on the flux deviation, it inherits the fundamental stability guarantees established in these

works. A complete Lyapunov derivation for the dual-parameter R_s and R_r adaptation will be addressed in future research.

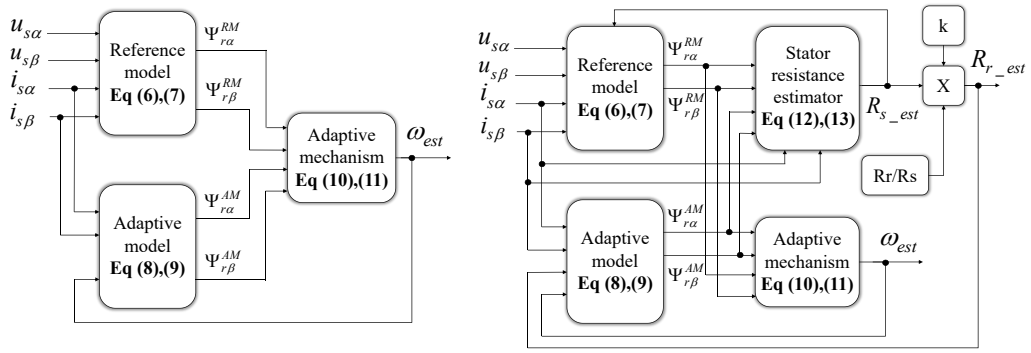

Figure 2. *Rotor flux-based model reference adaptive system structure.*
a) RF-MRAS without resistance estimator; b) RF-MRAS with resistance estimator.

Figure 2 illustrates the complete structure of the RF-MRAS. Specifically, figure 2a shows the RF-MRAS without integrating the R_s and R_r estimation blocks, while figure 2b presents the proposed RF-MRAS method with these components included.

3. RESULTS AND DISCUSSION

In this section, the control object is a three-phase squirrel cage induction motor with the following parameters: R_s = 3.179 (Ω); R_r = 2.118 (Ω); L_s = 0.209 (H); L_r = 0.209 (H); L_m = 0.192 (H); J = 0.047 (kg.m^2); p = 2; f = 50 (Hz); n_{rated} = 1420 (rpm); P_{rated} = 2.2 (kW). The results are analyzed and evaluated using MATLAB and Simulink.

All parameter limits used in the simulations, such as current, voltage, speed, and flux boundaries, were selected within the standard operating range of the tested induction motor to ensure consistent and realistic transient behavior.

This study is organized into two simulation cases, described in detail in table 1:

Table 1. *Simulation cases description.*

Case study	Scenario	Reference speed	Stator and rotor resistance estimator	R_s and R_r
1	1	Constant	No	---
	2	Constant	Yes	With proportion (k=1)
2	1	Variable	No	---
	2	Variable	Yes	With proportion (k=1)
3	1	Variable	No	---
	2	Variable	Yes	Without proportion (k=0.92308)

3.1. Case study 1

In case 1 - Simulation scenario 1, the reference speed is accelerated from 0 to 400 rpm within the first 0.5 seconds and then maintained constant at 400 rpm, as illustrated in figure 3c.

At 1.5 seconds and 2.5 seconds, the stator and rotor resistances of the motor are increased by 15% and 30%, respectively (figures 3a and 3b). In the scenario without the resistance estimator, the estimated motor speed is unstable, causing the actual motor speed to deviate from the reference. The estimated speed fluctuates between 389 rpm and 410 rpm, demonstrating that variations in stator and rotor resistances significantly affect the accuracy of the RF-MRAS speed estimation process.

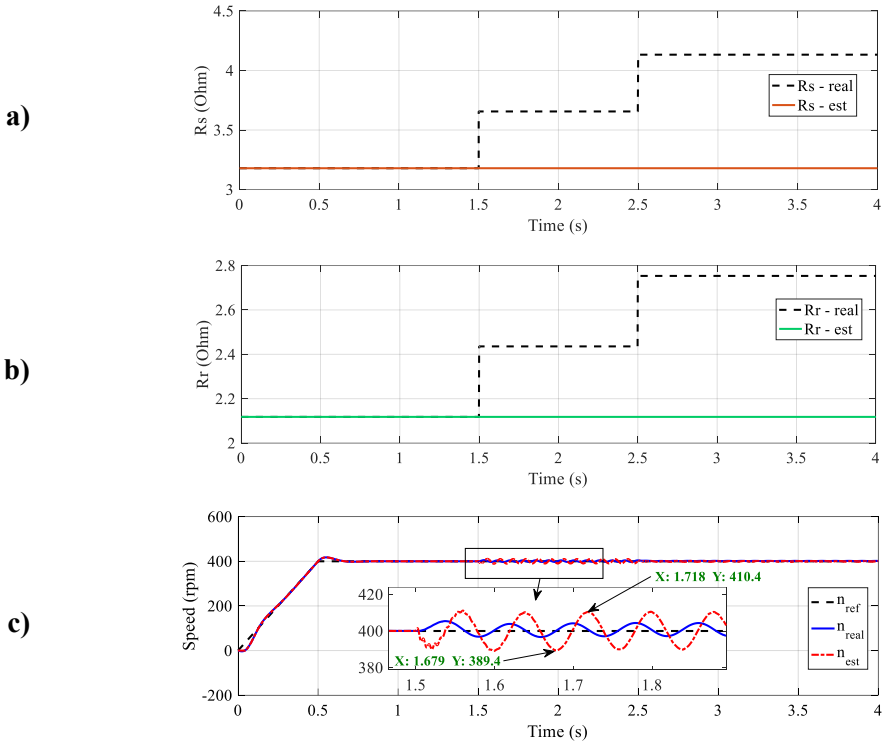

Figure 3. *Simulation results of case 1 without the resistance estimator. a) Stator resistance; b) Rotor resistance; c) Rotor speed.*

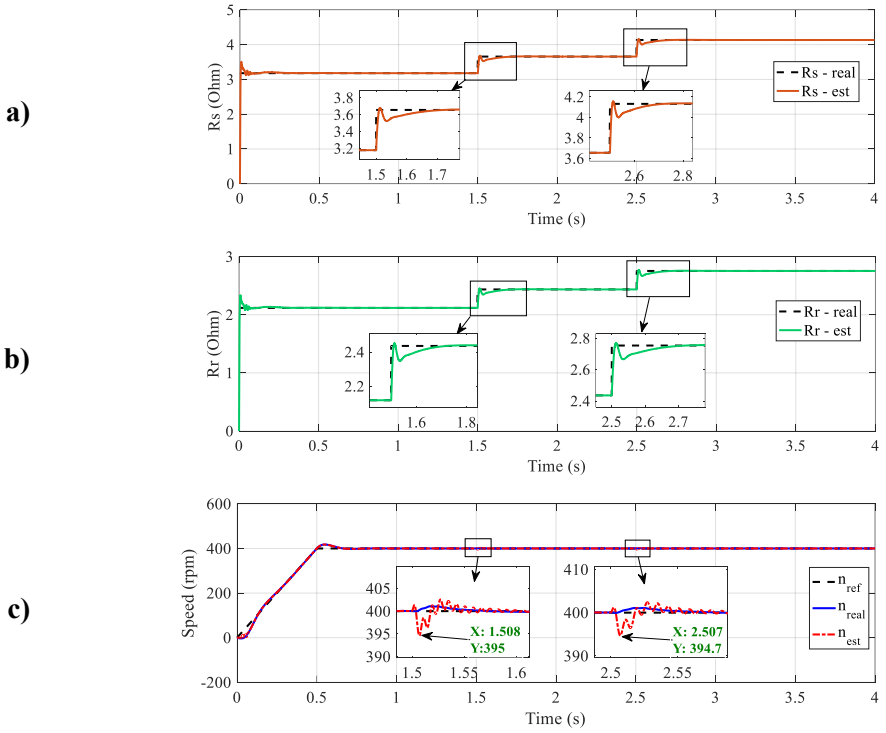

Figure 4. *Simulation results of case 1 with the resistance estimator. a) Stator resistance; b) Rotor resistance; c) Rotor speed.*

In case 1 - Simulation scenario 2, setting the reference speed is identical to that of Scenario 1. However, in this case, the system incorporates an online estimation block for both the stator and rotor resistances. At 1.5 seconds and 2.5 seconds, when the stator and rotor resistances suddenly increase, the adaptive estimation mechanism is activated. The estimated stator and rotor resistances closely follow their actual values, as shown in figures 4a and 4b. The estimated motor speed (figure 4c) fluctuated slightly during the transient period when the resistance increased, then quickly reached a steady state and closely followed the reference speed.

3.2. Case study 2

In case 2 - Simulation scenario 1, the reference speed is continuously varied to evaluate the stability and dynamic performance of the proposed method. The reference speed accelerates from 0 to 300 rpm within the first 0.5 seconds and then remains constant. Between 1.0 and 1.5 seconds, the reference speed decreases from 300 rpm to 100 rpm, and subsequently increases again at 2.0 seconds, forming a reference speed variation as shown in figure 5c.

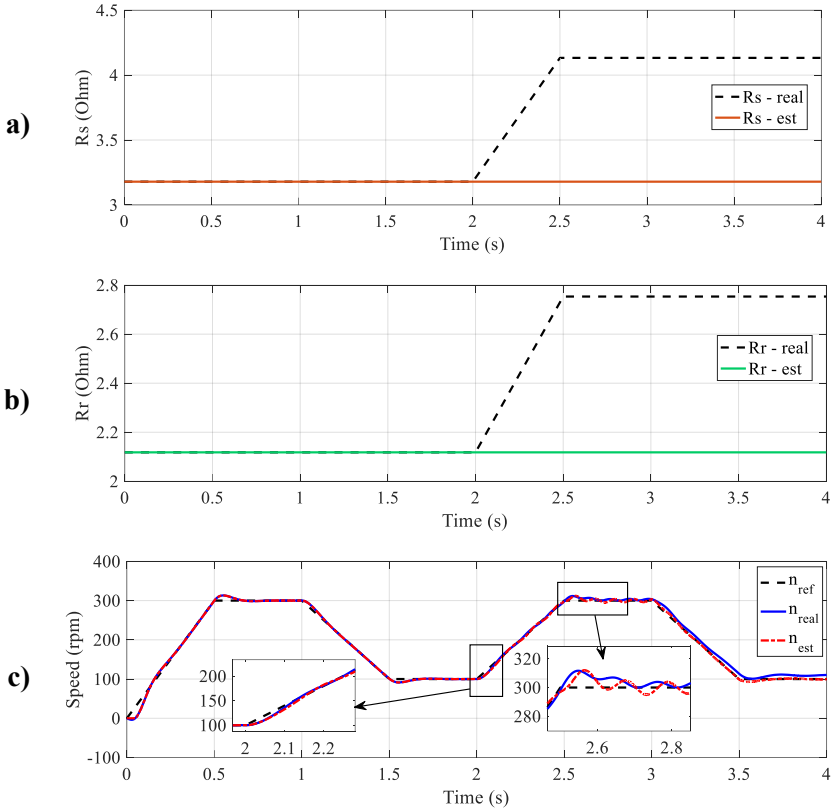

Figure 5. *Simulation results of case 2 without the resistance estimator. a) Stator resistance; b) Rotor resistance; c) Rotor speed.*

At 2.0 seconds, both the stator and rotor resistances increase gradually by 30% in a ramp manner (figures 5a and 5b). Similarly, in the case without the resistance estimation block, the estimated speed from the RF-MRAS observer is unstable, leading to instability in the overall system.

In case 2 - Simulation scenario 2, the system includes an estimation block for both stator and rotor resistances. Figures 6a and 6b show that the estimated stator and rotor resistances closely match the motor's actual resistance values. As a result, both the estimated and actual rotor speeds remain stable and operate smoothly (figure 6c).

a)

b)

c)

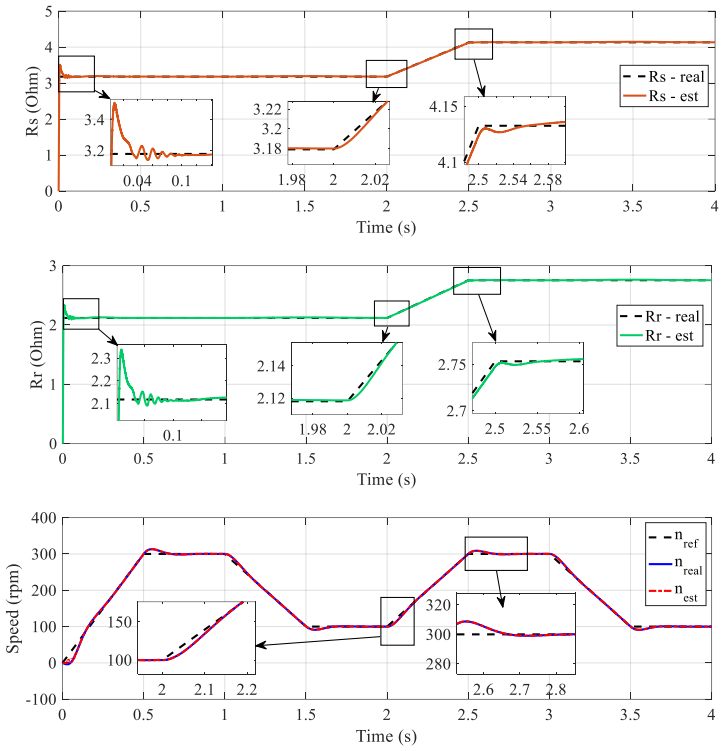

Figure 6. *Simulation results of case 2 with the resistance estimator. a) Stator resistance; b) Rotor resistance; c) Rotor speed.*

3.3. Case study 3

a)

b)

c)

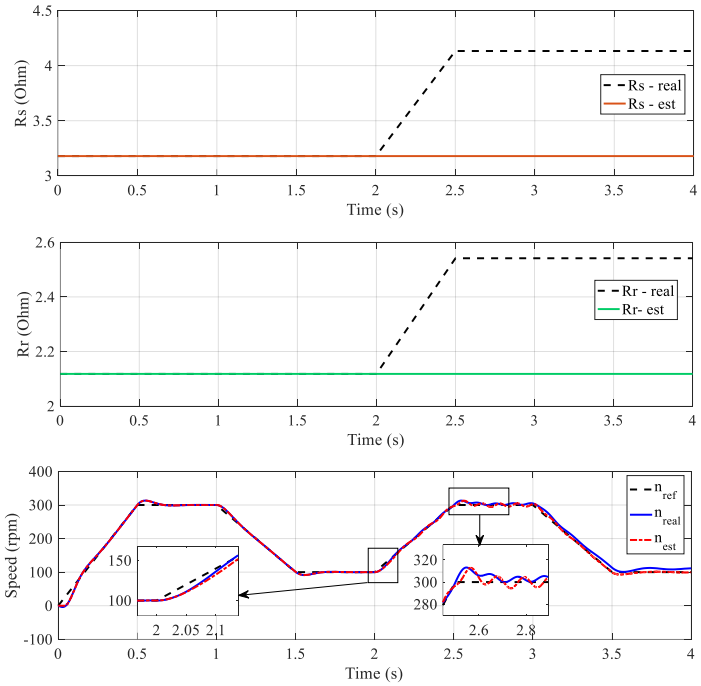

Figure 7. *Simulation results of case 3 without the resistance estimator. a) Stator resistance; b) Rotor resistance; c) Rotor speed.*

To evaluate the effectiveness of the RF-MRAS estimation block in various conditions, the authors additionally simulate the case in which the rotor resistance does not increase proportionally to the stator resistance. Depending on the structure of each motor type, the authors assume that in this case, the rotor bars are cooler than the stator windings; therefore, the stator resistance increases by 30%, and the rotor resistance increases by only 20%.

In case 3 - Simulation scenario 1, as the motor resistances increase, both estimated and actual motor speeds become unstable, similar to the behavior observed in the previous simulation cases.

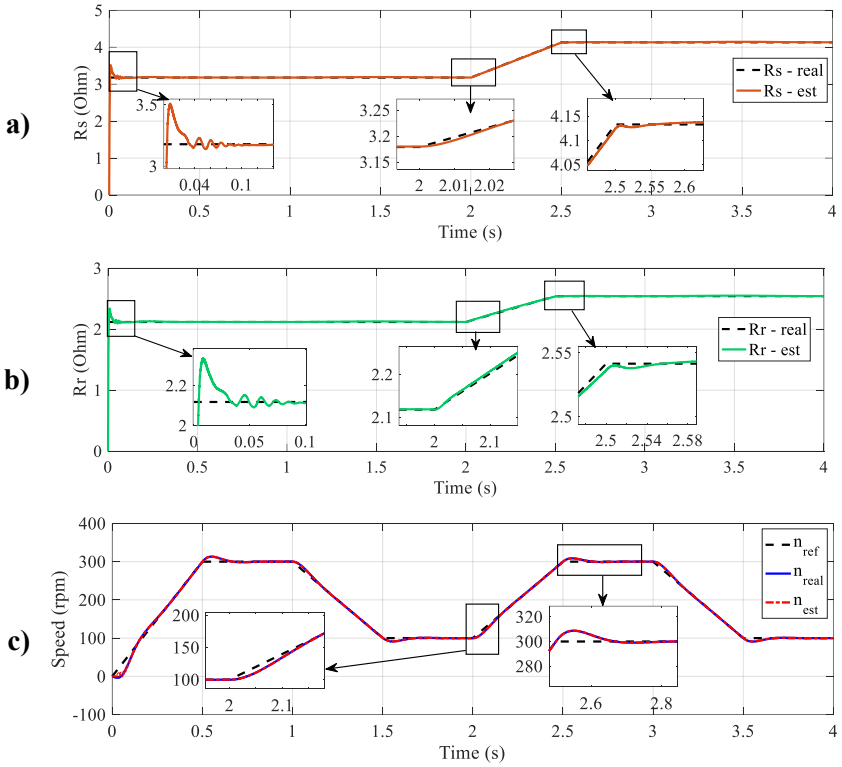

Figure 8. *Simulation results of case 3 with the resistance estimator. a) Stator resistance; b) Rotor resistance; c) Rotor speed.*

In Case 3 - Simulation scenario 2, the system includes an estimation block for both stator and rotor resistances. At 2 seconds, the stator resistance increases by 30%, and the rotor resistance increases by 20%. Figures 8a and 8b show that both the estimated stator and rotor resistances still follow the actual values. As a result, both the estimated and actual rotor speeds remain stable and operate smoothly (figure 8c).

3.4. Comparison between the proposed RF-MRAS method and related MRAS techniques

Table 2. *Summary and comparison among MRAS techniques.*

Criteria	RF-MRAS	CB-MRAS^{CV} [12]	CB-MRAS^{CC} [13]
ε	$\varepsilon^{RF} = \psi_{r\beta}.\hat{\psi}_{r\alpha} - \psi_{r\alpha}.\hat{\psi}_{r\beta}$	$\varepsilon^{CV} = \hat{\psi}_{r\beta}.\varepsilon_{i\alpha} - \hat{\psi}_{r\alpha}.\varepsilon_{i\beta}$	$\varepsilon^{CC} = \hat{\psi}_{r\beta}.\varepsilon_{i\alpha} - \hat{\psi}_{r\alpha}.\varepsilon_{i\beta}$
Estimated parameters	Speed, R_s, R_r	Speed and R_s	Speed and flux; no resistance estimation
Implementation complexity	Low - simple PI adaptation + proportional R_r inference	Medium - requires virtual current computation	Medium - requires stator-current estimator + current model

A comparative evaluation between the proposed RF-MRAS method and two related MRAS structures, namely the improved CB-MRAS^{CV} with estimated stator resistance [12] and the CB-MRAS^{CC} with formal stability analysis [13], is summarized in table 2.

4. CONCLUSIONS

This paper proposes an improved speed-sensorless FOC scheme for a three-phase induction motor using an adaptive RF-MRAS structure. The stator resistance was adaptively estimated from the flux deviation between the reference and adaptive models, while the rotor resistance was derived proportionally. The main contribution lies in the real-time estimation of stator and rotor resistances, effectively compensating for temperature-dependent variations that degrade conventional MRAS performance. Simulation results verified that the proposed method enhances speed estimation accuracy and stability under thermal variations. Although the approach has been validated through simulation, experimental testing has not yet been conducted, which is a current limitation of this study. In future work, the method will be implemented on a DSP/FPGA-based platform for real-time verification and further extended to incorporate iron-loss effects and potential applications in fault-tolerant motor control.

Acknowledgement: *This research is funded by Ton Duc Thang University.*

APPENDIX

Table 3. *Nomenclature.*

Symbol	Description	Symbol	Description
$\hat{u}_s$	Complex stator voltage	L_m	Magnetizing inductance
$\hat{i}_s, \hat{i}_r$	Complex stator and rotor current	$\omega_r = p\omega_m$	Rotor speed
$\hat{\psi}_s$, $\hat{\psi}_r$	Complex stator and rotor flux	T_L	Load torque
R_s, R_r	Stator and rotor resistance	T_e	Electromagnetic torque
L_s, L_r	Stator and rotor inductance	J	Moment of inertia

REFERENCES

[1]. C. D. Tran, M. Kuchar, V. Sotola, and P. D. Nguyen, *"Fault-tolerant control based on current space vectors against total sensor failures"*, Sensors, Vol. 24, No. 11, pp. 3558, (2024).

[2]. M. Masiala, B. Vafakhah, J. Salmon, and A. M. Knight, *"Fuzzy self-tuning speed control of an indirect field-oriented control induction motor drive"*, IEEE Trans. on Industry Applications, Vol. 44, No. 6, pp. 1732-1740, (2008).

[3]. L. Amezquita-Brooks, J. Liceaga-Castro, and E. Liceaga-Castro, *"Speed and position controllers using indirect field-oriented control: A classical control approach"*, IEEE Trans. on Industrial Electronics, Vol. 61, No. 4, pp. 1928-1943, (2013).

[4]. M. S. Zaky, M. M. Khater, H. Yasin, S. S. Shokralla, and A. El-Sabbe, *"Speed-sensorless control of induction motor drives"*, Eng. Res. J., Vol. 30, No. 4, pp. 433-444, (2007).

[5]. B. H. Dinh and C. D. Tran, *"Improved scalar control based on slip compensation from virtual speeds in three-phase induction motor drives"*, Int. J. of Power Electronics and Drive Systems (IJPEDS), Vol. 15, No. 3, pp. 1410-1416, (2024).

[6]. M. H. Bierhoff, *"A general PLL-type algorithm for speed sensorless control of electrical drives"*, IEEE Trans. on Industrial Electronics, Vol. 64, No. 12, pp. 9253-9260, (2017).

[7]. M. Korzonek, G. Tarchala, and T. Orlowska-Kowalska, *"A review on MRAS-type speed estimators for reliable and efficient induction motor drives"*, ISA Transactions, Vol. 93, pp. 1-13, (2019).

[8]. R. Kumar, S. Das, P. Syam, and A. K. Chattopadhyay, *"Review on model reference adaptive system for sensorless vector control of induction motor drives"*, IET Electric Power Applications, Vol. 9, No. 7, pp. 496-511, (2015).

[9]. A. R. Teja, V. Verma, and C. Chakraborty, *"A new formulation of reactive-power-based model reference adaptive system for sensorless induction motor drive"*, IEEE Trans. on Industrial Electronics, Vol. 62, No. 11, pp. 6797-6808, (2015).
[10]. N. Smith, S. M. Gadoue, and J. W. Finch, *"Improved rotor flux estimation at low speeds for torque MRAS-based sensorless induction motor drives"*, IEEE Trans. on Energy Conversion, Vol. 31, No. 1, pp. 270-282, (2015).
[11]. M. Adamczyk and T. Orlowska-Kowalska, *"Online stator and rotor resistance estimation for current sensor fault-tolerant control of induction motor drives"*, Proc. of the Int. Conf. on Electrical Drives and Power Electronics (EDPE), pp. 1-6, (2023).
[12]. Tran, P. Brandstetter, M. Kuchar, and P. Nguyen, *"An improved CB-MRAS using voltage model integrating stator resistance estimation in induction motor drives"*, Int. Review of Electrical Engineering (IREE), Vol. 19, No. 6, pp. 446-452, (2024).
[13]. T. Orlowska-Kowalska and M. Dybkowski, *"Stator-current-based MRAS estimator for a wide range speed-sensorless induction-motor drive"*, IEEE Trans. on Industrial Electronics, Vol. 57, No. 4, pp. 1296-1308, (2009).
[14]. A. Elhaj, M. Alzayed, and H. Chaoui, *"Multiparameter estimation-based sensorless adaptive direct voltage MTPA control for IPMSM using fuzzy logic MRAS"*, Machines, Vol. 11, No. 9, pp. 861, (2023).
[15]. Z. Zhang, G. Wang, Z. Wang, Q. Liu, and K. Wang, *"Neural network based Q-MRAS method for speed estimation of linear induction motor"*, Measurement, Vol. 205, pp. 112203, (2022).
[16]. Lu, W. Shan, Z. Yun, and W. Cao, *"PSO-optimized fuzzy MRAS control for permanent magnet synchronous motorized spindle"*, J. of Physics: Conf. Series, Vol. 2803, No. 1, pp. 012004, (2024).
[17]. V. R. Jevremovic, V. Vasic, D. P. Marcetic, and B. Jeftenic, *"Speed-sensorless control of induction motor based on reactive power with rotor time constant identification"*, IET Electric Power Applications, Vol. 4, No. 6, pp. 462-473, (2010).
[18]. S. Maiti, C. Chakraborty, Y. Hori, and M. C. Ta, *"Model reference adaptive controller-based rotor resistance and speed estimation techniques for vector controlled induction motor drive utilizing reactive power"*, IEEE Transactions on Industrial Electronics, Vol. 55, No. 2, pp. 594-601, (2008).
[19]. P. Cao, X. Zhang, and S. Yang, *"A unified-model-based analysis of MRAS for online rotor time constant estimation in an induction motor drive"*, IEEE Transactions on Industrial Electronics, Vol. 64, No. 6, pp. 4361-4371, (2017).

TÓM TẮT

MRAS nâng cao với bộ ước tính điện trở stator và rotor trong điều khiển vector động cơ không đồng bộ

Nghiên cứu này tập trung vào vấn đề suy giảm độ chính xác ước lượng tốc độ trong hệ truyền động động cơ không đồng bộ điều khiển không cảm biến tốc độ, vốn bắt nguồn từ sự thay đổi của điện trở stator và rotor theo nhiệt độ. Sự biến thiên của các tham số này ảnh hưởng đáng kể đến bộ quan sát RF-MRAS, dẫn đến suy giảm độ bền vững và tiềm ẩn nguy cơ mất ổn định trong các điều kiện quá độ. Để khắc phục hạn chế này, bài báo đề xuất một cấu trúc điều khiển tựa từ thông rotor (FOC) cải tiến, tích hợp bộ quan sát RF-MRAS thích nghi với cơ chế ước lượng trực tuyến điện trở stator và suy luận tỷ lệ điện trở rotor. Mô hình động cơ được xây dựng trên hệ tọa độ tĩnh α-β và sau đó biến đổi sang hệ tọa độ quay d-q để triển khai điều khiển vectơ. Các trường hợp mô phỏng đa dạng chứng minh phương pháp đề xuất giúp nâng cao đáng kể độ chính xác ước lượng tốc độ và cải thiện độ ổn định tổng thể của hệ thống. Nhờ cấu trúc đơn giản và không yêu cầu tính toán phức tạp, phương pháp này phù hợp cho các nền tảng điều khiển thời gian thực trong hệ truyền động không cảm biến hiện đại.

Từ khoá: Động cơ không đồng bộ; Điều khiển tựa từ thông; Không cảm biến tốc độ; RF-MRAS; Biến thiên điện trở.